



Sensitivity of design parameters on the stability of apex connections in cold-formed steel portal frames

Hannah B. Blum¹, Zhanjie Li²

Abstract

Cold-formed steel portal frames have joints that are typically connected by bolting the main frame members and connection brackets together for apex, eaves, and knee connections, if applicable. The strength and stiffness of connections have a significant impact on frame capacity and behavior and affect the internal force and moment distributions and deflections. The apex connection, formed by brackets bolted to lipped-channel rafters, has been shown to fail by buckling of the apex bracket plate at loads lower than the capacity of the main frame members. Previously, an advanced finite element model was created and validated with experimental results from a series of apex connection tests, which showed a change in moment-rotation behavior depending on the size and thickness of the connected parts. Parametric studies were conducted using the validated finite element model to further investigate the effect of the connection input parameters on the strength and stiffness of the overall connection. The effects of combinations of the rafter thickness and apex bracket thickness on the connection moment-rotation behavior, stiffness, and strength were examined for apex connections formed from C150 and C200 lipped channel rafters with corresponding brackets. Recommendations for apex connection design improvement is discussed.

1. Introduction

Portal frames are commonly used to provide large open spaces for industrial, farming, and residential purposes. Traditionally, portal frames are composed of hot-rolled steel sections. There are several benefits to using cold-formed steel sections, including reduced material, fabrication, transport, and construction costs, and a higher strength to weight ratio compared to hot-rolled steel. However, cold-formed steel structures cannot be constructed or analyzed using the same methods as hot-rolled steel structures as they are prone to local and distortional buckling, as well as global buckling, and the interaction of these buckling modes. Additionally, as the elements are thin, connections in cold-formed steel portal frames are usually formed through mechanical fastening or interlock, such as bolting of plates or brackets in between the channel sections, as opposed to welded connections in their hot-rolled counterparts. These cold-formed steel

¹ Assistant Professor, Department of Civil & Environmental Engineering, University of Wisconsin-Madison, Hannah.blum@wisc.edu

² Associate Professor, Department of Engineering, SUNY Polytechnic Institute, Utica, NY, Zhanjie.li@sunypoly.edu

connections are found to be semi-rigid [1]. The internal actions and deflections of portal frames are affected by the connection stiffness and behavior, and therefore it is important to correctly quantify connection strength and stiffness to accurately determine portal frame behavior. The apex connection of a portal frame is where the two rafter sides are connected and is sometimes referred to as the ridge of the portal frame.

Finite element modeling has been previously used for parametric studies of portal frames to determine the effects of various components on the frame. A parametric study was used to determine the effect of knee braces with pinned or rigid connections at the joints to frames with rigid joints only [2], and to study the effects of the size of the connection brackets [3] and bolt group length [4]. A parametric study was completed to determine if frames designed based on a rigid and full strength joint assumptions were safe under gravity load [5].

To study the effects of the connection properties on the strength and stiffness of cold-formed steel apex connections, a series of finite element parametric studies were conducted. One study varied only the thickness of the lipped channel rafter section, and another study varied only the thickness of the apex bracket. As apex connection stiffness affects the overall deflection in the frame, it is crucial to study this connection.

2. Background

This parametric study was validated by previous experimental studies on the apex connection. A series of twelve tests on the apex connections of cold-formed steel portal frames has been conducted [6]. The rafters consisted of back-to-back lipped channels bolted together through the webs, and the apex brackets consisted of back-to-back lipped L-brackets bolted through the webs. Various channel sizes and thickness were tested, including section depths of 203 mm with a thickness of either 1.5, 1.9, or 2.4 mm, and section depths of 152 mm with a thickness of 1.5, 1.9, or 2.4 mm. There were two apex bracket sizes: one for the 203 mm depth channels, and one for the 152 mm depth channels, both of which were 2.4 mm thick. The apex connection specimens were approximately 2 m long. The channel and apex brackets were bolted together with grade 8.8 M14 bolts for the C150 tests, and M16 bolts for the C200 tests. At other locations, the channels were bolted together with grade 4.6 M12 bolts with integrated washers. The channels and the apex brackets were fabricated using G450 steel, which indicates a nominal minimum yield stress of 450 MPa. Coupon tests from the channels and brackets were conducted according to the Australian Standard [7] and it was found that the material had an average Young's Modulus of 206 GPa and an average 0.2% proof stress of 508 MPa. Further details are given elsewhere [6].

The in-plane moment-rotation behavior of all specimens was recorded for each test. All specimens failed by buckling of the apex bracket and no visible bolt-hole elongation or bolt-slip was visible. The C150-15, C150-19, C200-15, and C200-19 specimens showed a rounded moment-rotation behavior after an initial linear elastic region. The C150-24 and C200-24 specimens showed a bi-linear moment-rotation behavior prior to reaching peak strength, although this behavior was not fully obvious for the C200-24. It was hypothesized that the overall stiffness behavior of the connection was affected by the ratio of the geometric stiffness of the rafter to bracket. Specimens with low ratios showed an early reduction in overall connection stiffness than specimens with higher ratios. As loading increases, it becomes easier for the apex

bracket to deflect rather than bending in the rafters or in the combined system, which results in an earlier loss of stiffness in the connection compared to the specimens with higher $I_{X, \text{bracket}}$ to $I_{X, \text{rafter}}$ ratios [6]. Full details of the experimental setup and results are given elsewhere [8], [9].

Finite element models of the connections tested in [6] were created and compared against the experimental results and showed good comparisons, as shown in Fig. 1 [10]. Section 3 describes the model details for the parametric study, however for the validation of the finite element analysis, measured dimensions and thicknesses of the channel sections and apex brackets were used in the models. Further details of the validation study are given elsewhere [10].

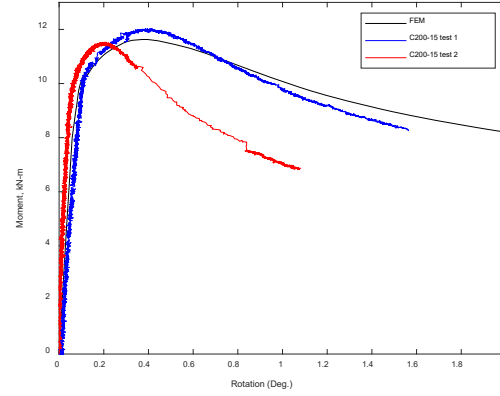


Figure 1: Moment vs. rotation for C200-15 from [10]

3. Model details

Advanced shell finite element models were created in ABAQUS [11] of the apex connections. Nominal dimensions are given in Table 1, and complete dimensions of the apex brackets are given in [6]. The model was first created in SolidWorks and then the geometry was imported into ABAQUS. The channel sections and apex brackets were modeled with 4-node doubly curved shell elements with linear interpolation, reduced integration and hourglass control (S4R elements). Bolts in the connections were modeled using multi-point-based coupling constraints (MPC beam). This uses distributed coupling constraints to connect the faces of elements through either couplings or connectors [12]. First, an attachment point was defined at the location of a bolt, which was projected through the specified numbers of layers in a specified direction to connect the members at the location of the bolt. The physical radius of the connector was specified in the fastener definition and was equal to the radius of the bolt. A rigid beam multi point constraint was chosen to model the bolts assuming the bolts were sufficiently tight and there was no bolt slip. Structural distributing was chosen as the fastener formulation, which couples the displacements and rotations of the fastening points to the average displacement and rotation of the nodes. All bolts were modeled in this manner. Contact and friction were modeled between the webs of back-to-back apex brackets and channel sections. Hard contact was defined in the normal direction, and a coefficient of friction of 0.5 in the tangent direction. The material properties of the channels and apex connection brackets were modeled as an elastic perfectly curve with a Young's Modulus of 206 GPa and a 0.2% proof stress of 508 MPa, as measured during tensile coupon tests [8], [9]. The stress and strain was converted to true stress and true strain and inputted into the material property definitions in ABAQUS [11].

The ends of the rafters are restrained against twist along the longitudinal axis of the rafter by analytically tying all the nodes at the ends and restraining the corresponding twist degree of freedom. To simulate a roller support, the rafter ends are restrained from lateral displacements but allow longitudinal displacement. The nodes at the locations of the purlin brackets in the experiments were restrained in the out-of-plane direction to represent these supports. To prevent rigid body motion of the connection, several nodes in the center of the apex bracket were

restrained from moving horizontally. A rigid body was created by tying all the nodes at the location of the loading pin hole (in the experiments) to the center of the hole and then the prescribed displacement was applied at the center reference node. This permitted the displacement-controlled loading method. To consider the effects of the imperfections resulting from offsets in the testing rig, an initial displacement was introduced on the loading application reference node, which essentially modeled potential offsets introduced when placing a specimen inside a testing rig. This also helped to promote convergence of the initial perfect model. The imperfections were equal and opposite in sign, being -1 mm at the left-side loading plate and +1 mm at the right-side loading plate. This initial displacement step was analyzed first using the static, general method before vertical load was applied.

A geometric and material nonlinear static analysis was completed. Due to the convergence issue of the contact modeling, the analysis was a general static analysis with stabilization by displacement control. Residual stresses were not modeled as the through-thickness residual stress is accounted for in the finite element models through the measured stress-strain curve determined from coupon tests, and membrane residual stresses are small relative to the yield stress in cold-formed steel sections [13]. The mesh size was approximately 8 mm for all rafter members and 6 for all bracket members in the connection. The layout of the finite element model with rafter channels and apex brackets for a C150 specimen is shown in Fig. 2.

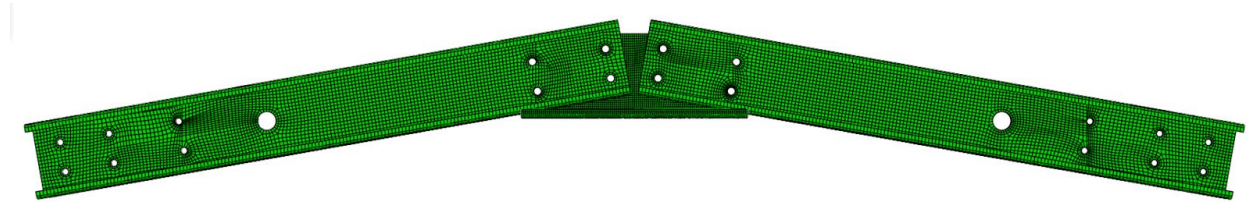


Figure 2: FEM of a C150 apex connection

4. Parametric Studies

Moment-rotation results were determined from all finite element model results. The rotations at each side of the apex connection were averaged, and the vertical reaction forces, from which to calculate the applied moment, from each side of the connection were averaged. Therefore, the presented results are the average moment-rotation results of the connection.

4.1 Rafter thickness

The effect of changing the thickness of the lipped channel rafter was investigated. The currently available lipped channel sizes have the same web and flange dimensions for all members with the same nominal web depth, but the lip dimension changes with the thickness of the member. Therefore, for a realistic analysis, the lip length was interpolated between known dimensions (available) for the hypothetical (estimated) rafter section sizes. The nominal dimensions of all the connection members are given in Table 1.

The moment-rotation plots of all C150 connections are given in Fig. 3. Two distinct failure modes are visible as shown between the left and right plots in the figure. The lipped channel rafters did not experience any buckling for all FEA results. This apex failure mode can be further

investigated by observing the buckled shape of the apex brackets, as shown in Fig. 4 for an isometric view and Fig. 5 for a view from the top. Both Figs. 4 and 5 compared the buckled shape of the apex brackets for a C150-21 (left and top in figures) and C150-30 (right and bottom in figures) apex connections. The C150-21 apex bracket failure mode caused each side of the apex connection to move out-of-plane of the connection in alternating directions. However, the C150-30 apex brackets failed in the center of each apex bracket in the region in-between the rafters, by buckling independently out of plane. The difference in failure mode is reflected in the moment-rotation curves in Fig. 3.

Table 1: Dimensions and thickness of connected members in the apex connections

Channel	Channel dimensions (mm)			Apex bracket	
	web \times flange \times lip	t (mm)	available or estimated	Size	t (mm)
C200-15	203 \times 76 \times 15.5	1.5	available	C200	2.45
C200-17	203 \times 76 \times 16.5	1.7	estimated		
C200-19	203 \times 76 \times 19.0	1.9	available		
C200-21	203 \times 76 \times 17.4	2.1	estimated		
C200-24	203 \times 76 \times 21.0	2.4	available		
C200-26	203 \times 76 \times 21.7	2.6	estimated		
C200-30	203 \times 76 \times 23.6	3.0	estimated		
C150-15	152 \times 64 \times 15.5	1.5	available	C150	2.4
C150-17	152 \times 64 \times 16.0	1.7	estimated		
C150-19	152 \times 64 \times 16.5	1.9	available		
C150-21	152 \times 64 \times 17.4	2.1	estimated		
C150-24	152 \times 64 \times 18.5	2.4	estimated		
C150-30	152 \times 64 \times 22.0	3.0	estimated		

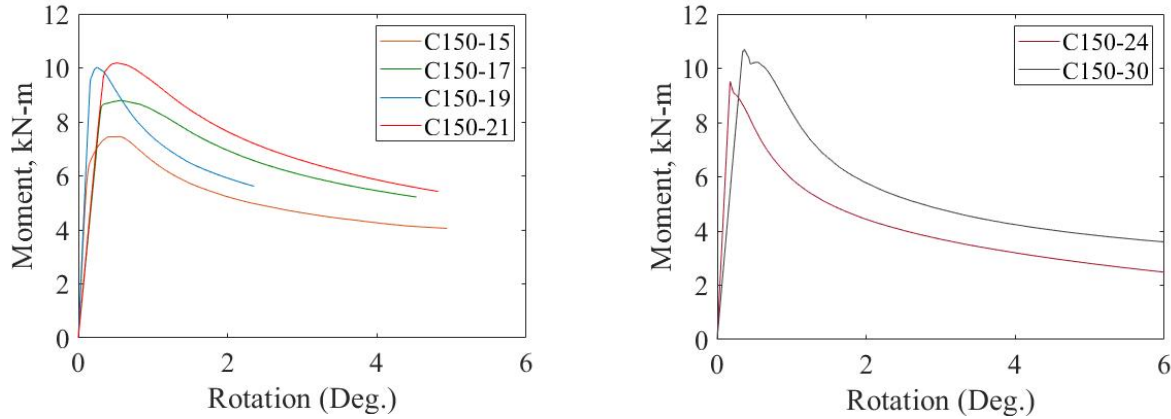


Figure 3: FE results of C150 connections with various rafter sizes; (left) thinner rafters and (right) thicker rafters

The moment-rotation plots of all C200 connections are given in Fig. 6. All model results show a similar moment-rotation behavior, and a trend of increasing strength with increasing rafter thickness. All results show the similar apex bracket buckling failure as shown in Fig. 7 for the C200-24 apex connection.

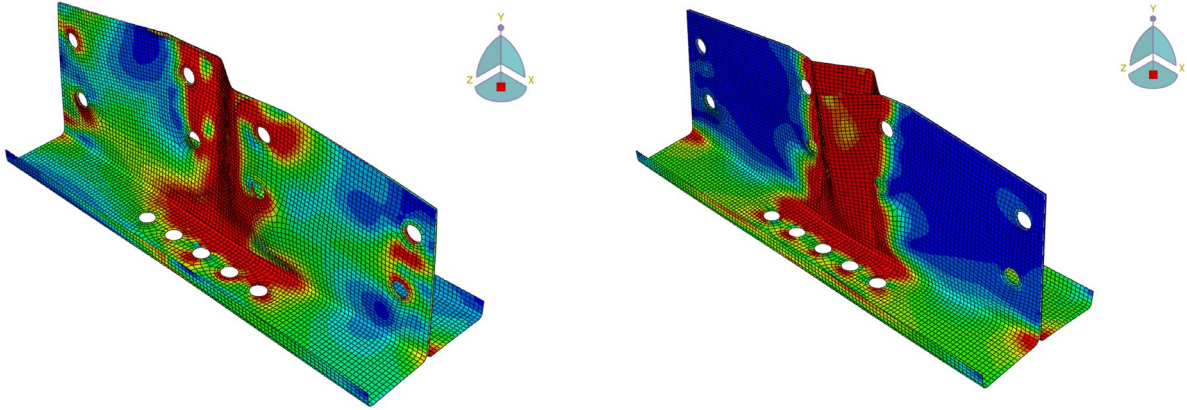


Figure 4: Apex bracket buckled shape isometric view; (left) C150-21 and (right) C150-30

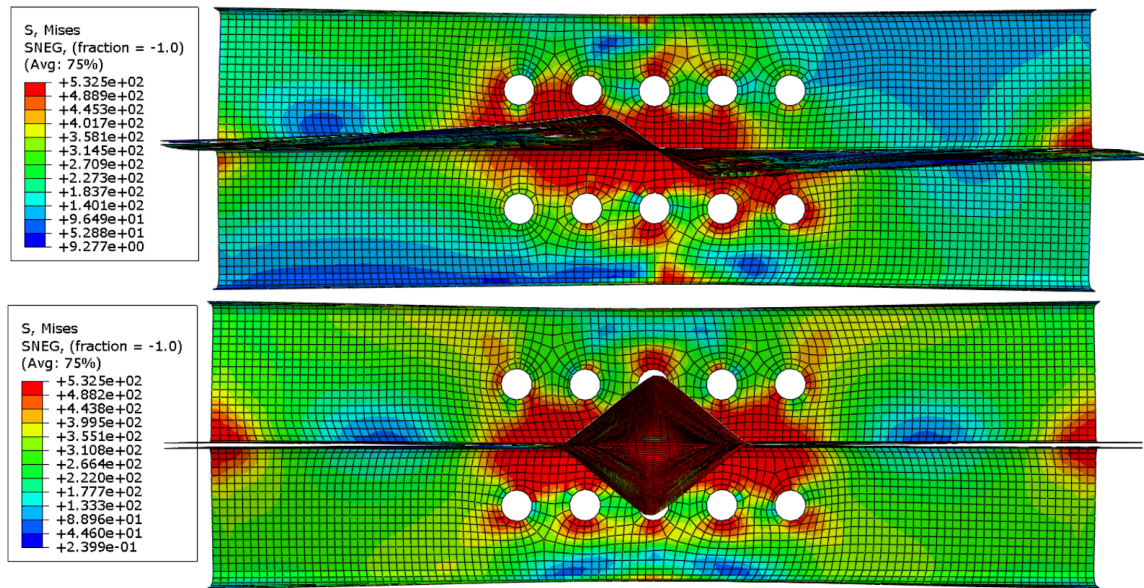


Figure 5: Apex bracket buckled shape top view with Von Mises stress contour; (top) C150-21 and (bottom) C150-30

4.2 Apex bracket thickness

The effect of changing the thickness of the apex bracket was investigated. The nominal section sizes given in Table 1 were modeled and only the thickness of bracket was changed. The original bracket thickness was 2.4 mm, and this was decreased to as low as 2.0 mm or increased to as high as 2.8 mm. The results of the C150 apex connections are given in Figs. 8, 9, and 10.

Overall, connections with thicker apex brackets show an increased strength, but not necessarily an increase in connection stiffness. For both the C150-19 and C150-24 connections, the 2.8 mm thick bracket resulted in a slightly less stiff connection than the connection with the 2.4 mm thick apex bracket. Of note is the unique behavior of the C150-24 apex connection with a bracket thickness of 2.8 mm, shown in Fig. 10. At around 10 kN-m there is a slight kink in the moment-rotation slope. Observing the apex bracket stress distribution in Fig. 11 provides some insight into this behavior. At the kink in the slope, one side of the apex connection is experiencing plastic behavior. The load continues to increase and at peak, both sides of the apex connection experience plastic behavior. This illustrates the complex failure mode of the apex connections.

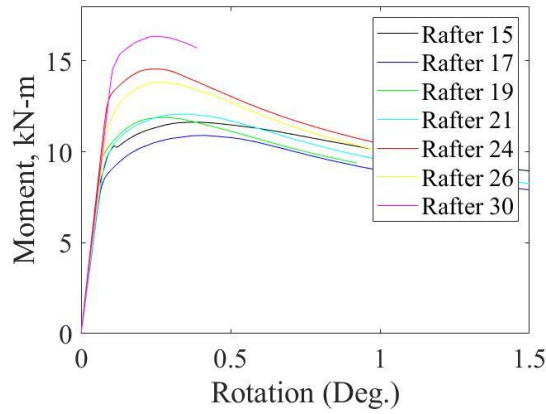


Figure 6: FE results of C200 connections with various rafter sizes

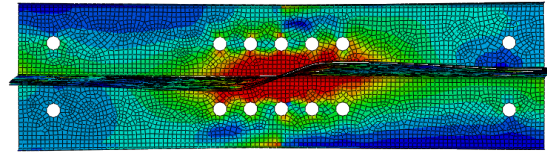


Figure 7: Apex bracket buckled shape for C200-24

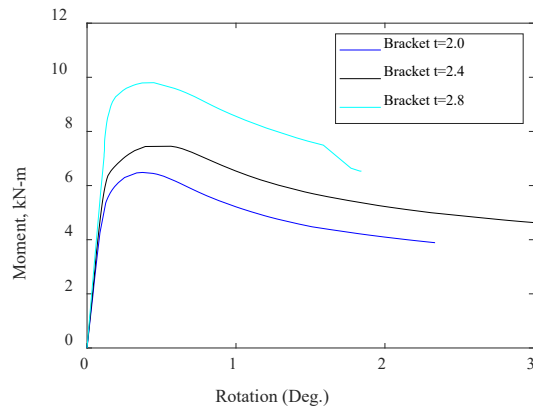


Figure 8: FE results of C150-15 apex connections with various bracket thicknesses

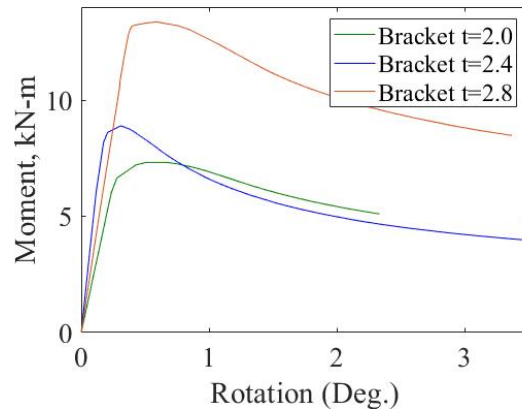


Figure 9: FE results of C150-19 apex connections with various bracket thicknesses

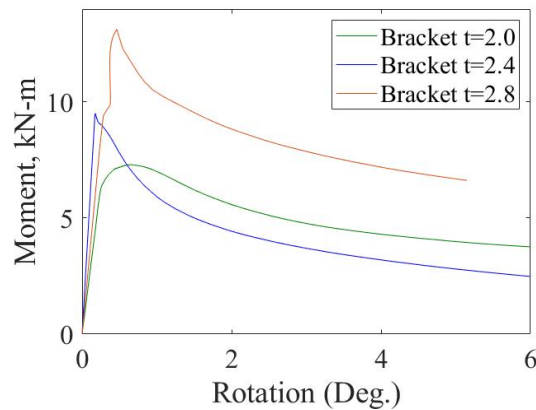


Figure 10: FE results of C150-24 apex connections with various bracket thicknesses

The results of the C200 apex connections are given in Figs. 12, 13, and 14. Overall, a thicker apex bracket resulted in a stronger connection, but the connection was less stiff than those connections with 2.45 mm thick apex brackets. This effect is shown in all C200 connections but is more pronounced in the C200-19 connections. Also of note is a slight kink in the curve for the

C200-24 connection with the 2.8 mm thick bracket. This is similar to the moment-rotation curve for the C150-24 connection with 2.8 mm thick brackets. Further investigations are recommended.

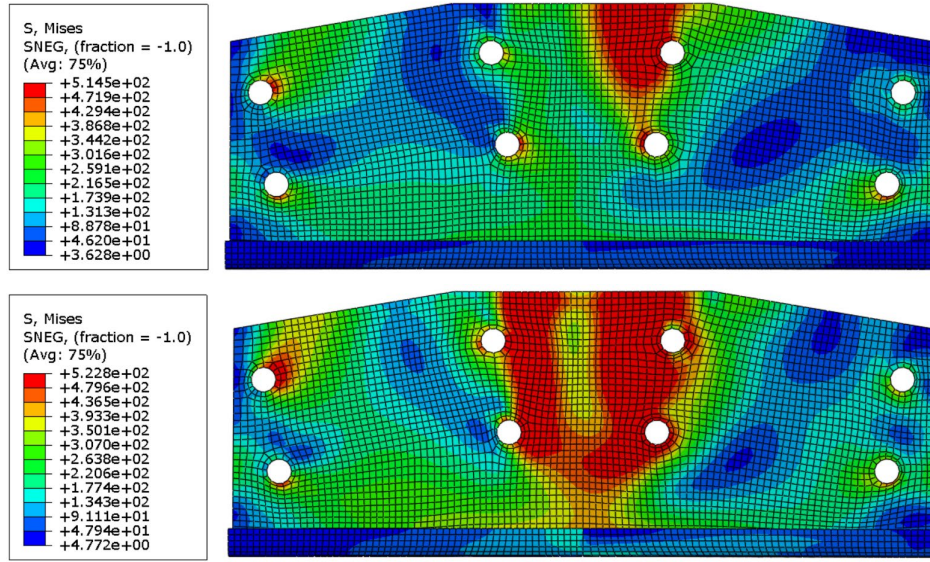


Figure 11: Apex bracket Von Mises stress for C150-24 connection with bracket $t=2.8$; (top) at start of kink in Figure 10, and (bottom) at peak load

5. Future work

Further parametric studies are planned which include investigating the effects of the apex bracket length and the addition of an apex bracket top flange. Additionally, the impact of imperfections on the apex bracket can be explored. This can be completed by imposing 1st order and 2nd order buckling mode imperfections on the initial geometry of the bracket, and then applying load to the connection. As the failure of this connection represents a computationally complex inelastic buckling behavior with contact interactions, further model refinements to improve convergence can be explored.

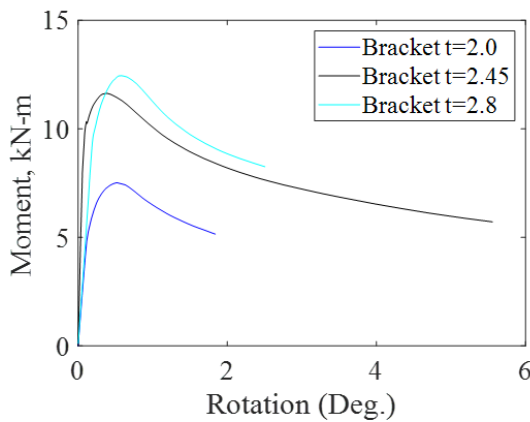


Figure 12: FE results of C200-15 apex connections with various bracket thicknesses

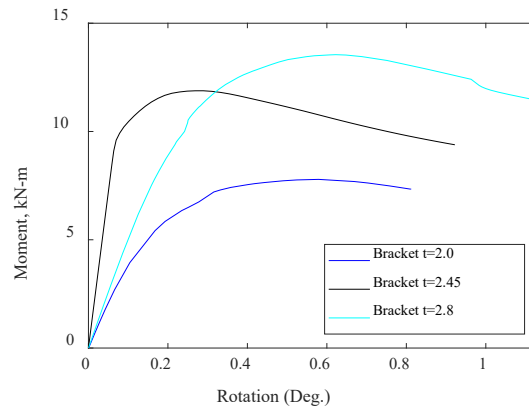


Figure 13: FE results of C200-19 apex connections with various bracket thicknesses

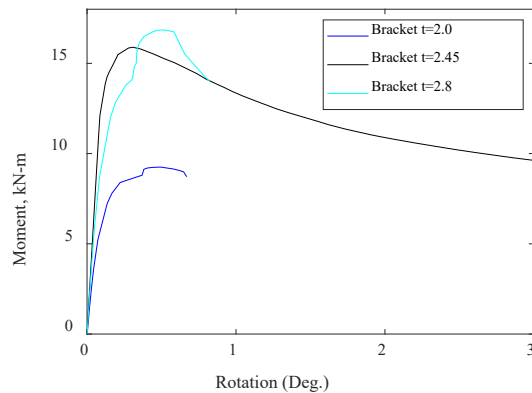


Figure 14: FE results of C200-24 apex connections with various bracket thicknesses

6. Conclusions

Finite element models have been created of cold-formed steel portal frame apex connections for various lipped channel rafter thicknesses, depths, and apex bracket sizes. The apex connections are formed by bolting the apex brackets back-to-back with the back-to-back rafter sections. Apex connections with nominal rafter depths of 150 mm and 200 mm were investigated. Parametric studies were conducted to study the effects of changing the thickness of the lipped channel rafter sections and the effects of changing the thickness of the apex brackets. In-plane bending moment versus apex rotation behavior of the finite element models were produced for the parametric studies to examine the effects of changing the component thickness on the strength and stiffness of the connection. All models showed a complex inelastic buckling failure mode of the apex connection bracket members.

References

- [1] W. K. Yu, K. F. Chung, and M. F. Wong, "Analysis of bolted moment connections in cold-formed steel beam-column sub-frames," *J. Constr. Steel Res.*, vol. 61, no. 9, pp. 1332–1352, Sep. 2005, doi: 10.1016/j.jcsr.2005.03.001.
- [2] A. M. Wrzesien and J. B. P. Lim, "Cold-formed steel portal frame joints : a review," in *Proceedings Nineteenth International Specialty Conference on Cold-Formed Steel Structures*, 2008, pp. 591–606.
- [3] J. B. P. Lim and D. A. Nethercot, "F.E.-assisted design of the eaves bracket of a cold-formed steel portal frame," *Steel Compos. Struct.*, vol. 2, no. 6, pp. 411–428, 2002.
- [4] S. M. Mojtabaei, J. Becque, and I. Hajirasouliha, "Local Buckling in Cold-Formed Steel Moment-Resisting Bolted Connections: Behavior, Capacity, and Design," *J. Struct. Eng.*, vol. 146, no. 9, p. 04020167, 2020, doi: 10.1061/(asce)st.1943-541x.0002730.
- [5] C. Jackson, A. M. Wrzesien, R. P. Johnston, A. Uzzaman, and J. B. P. Lim, "Effect of reduced joint strength and semi-rigid joints on cold-formed steel portal frames," in *Proceedings Sixth International Conference on Coupled Instabilities in Metal Structures*, 2012, pp. 287–294.
- [6] J. Peng, J. Bendit, and H. B. Blum, "Experimental study of apex connection stiffness and strength of cold-formed steel double channel portal frames," in *Proceedings Twentyfourth International Specialty Conference on Cold-Formed Steel Structures*, 2018.
- [7] AS 1391, *Australian Standards 1391: Metallic Materials - Tensile Testing at Ambient Temperature*. 2007.

- [8] J. Peng, “Experimental Investigation of Apex Connection Stiffness in Cold-Formed Steel Portal Frames,” The University of Sydney, 2017.
- [9] J. Bendit, “Experimental Investigation of Apex Connection Moment-Rotational Stiffness in Cold-Formed Steel Portal Frames,” The University of Sydney, 2017.
- [10] H. B. Blum and Z. Li, “Stability of apex connections in cold-formed steel portal frames,” in *Structural Stability Research Council Annual Stability Conference 2019, SSRC 2019*, 2019.
- [11] ABAQUS, “ABAQUS / Standard Version 6.14.” Dassault Systemes, Providence, RI, USA, 2014.
- [12] ABAQUS, *ABAQUS Documentation*. Providence, RI, USA: Dassault Systemes, 2014.
- [13] C. D. Moen, T. Igusa, and B. W. Schafer, “Prediction of residual stresses and strains in cold-formed steel members,” *Thin-Walled Struct.*, vol. 46, no. 11, pp. 1274–1289, 2008, doi: 10.1016/j.tws.2008.02.002.